Available online at www.sciencedirect.com

SCIENCE DIRECT®

Journal of Catalysis 234 (2005) 282–291

JOURNAL OF CATALYSIS

www.elsevier.com/locate/jcat

Can TiO_2 promote the reduction of nitrates in water?

Jacinto Sá [a,b], Thomas Berger [b], Karin Föttinger [b], Alexander Riss [b], James A. Anderson [a,*], Hannelore Vinek [b]

[a] Surface Chemistry and Catalysis Group, Department of Chemistry, University of Aberdeen, Meston Walk, Old Aberdeen AB24 3UE, UK
[b] Institute of Materials Chemistry, Vienna University of Technology, Veterinaerplatz 1, A-1210 Vienna, Austria

Received 10 June 2005; accepted 16 June 2005

Abstract

Monometallic palladium catalysts were synthesized using different titanium supports and tested for the reduction of nitrates from aqueous solutions using hydrogen as a reductant. The Pd/TiO_2 catalysts were characterized by electron paramagnetic resonance (EPR), low-temperature Fourier transform infrared (FTIR) spectroscopy of adsorbed CO, and X-ray diffraction (XRD). The catalysts studied exhibited a high activity for nitrate removal with a lower tendency for nitrite formation than the conventional bimetallic Pd catalysts. Although ammonium formation was greater than desired, the use of a monometallic catalyst for this two-step reduction process is significant and suggests that a single site may be responsible for both reduction stages. The titanium support (particularly the Ti^{3+} centers generated during prereduction in the presence of Pd) appear to play an important role in the nitrate degradation process. The potential role of Pd β-hydride in generating these Ti^{3+} centers is discussed.

Keywords: Pd/TiO_2; Low-temperature Fourier transform infrared spectroscopy; Nitrate reduction; Aqueous solutions

---

1. Introduction

The demand for good-quality water has increased with the increased extent of water usage; however, excessive application of nitrate fertilizers in agriculture can consequently lead to the leaching of nitrates into groundwater and hence into surface water. Nitrate levels above a certain concentration (50 ppm in the European Union [EU]) are deemed unacceptable. High nitrate concentrations in drinking water are harmful because of the reduction of nitrates to nitrites, which combine with hemoglobin in the blood to form methemoglobin; furthermore, nitrates can cause cancer and hypertension through nitrosamine formation [1].

The problem related to the contamination of groundwater is becoming more pronounced. The conclusion is based on the report of the European Environmental Agency released in 1998, which estimated that 87% of the agricultural lands in the EU have nitrate concentrations in groundwater exceeding the imposed guideline level (25 ppm).

From an environmental standpoint, one of the most acceptable methods of removing nitrates is to convert them to N_2. Liquid-phase nitrate hydrogenation over a catalyst appears to be one of the most attractive processes to achieve this [2–20]. Much of the research on catalytic reduction has focused on the use of bimetallic catalysts, but more recently, studies involving monometallic catalysts, (in particular, using semiconducting oxides as supports) have appeared [21,22].

As part of this strategy, the use of TiO_2 impregnated with Pd was investigated. These types of catalysts have been widely investigated in liquid-phase hydrogenation processes [23–26], of which nitrate reduction from aqueous solutions bears some relation. The catalysts were then submitted to pretreatments involving different reduction temperatures. The influences of these thermal treatments on the sample characteristics were evaluated by Fourier transform infrared (FTIR) spectroscopy using CO as a probe molecule and elec-

---

[*] Corresponding author.
E-mail address: j.anderson@abdn.ac.uk (J.A. Anderson).

0021-9517/$ – see front matter © 2005 Elsevier Inc. All rights reserved.
doi:10.1016/j.jcat.2005.06.015

tron paramagnetic resonance (EPR) at low temperature, and kinetic reactions were investigated using a standard batch reactor.

2. Experimental

TiO_2 P25 (P25) with a surface area of 49 m^2/g (N_2, 77 K, BET method [27]) support was supplied by Degussa, and the monocrystalline titania (anatase (Ana) with a surface area of 93 m^2/g (N_2, 77 K, BET method [27]) and rutile (Rut) with a surface area of 16 m^2/g (N_2, 77 K, BET method [27])) supports were self-prepared through chemical vapor deposition. Briefly, the TiO_2 particles were produced by means of thermal decomposition of titanium isopropoxide vapor in a flow reactor system by the metal organic chemical vapor deposition method [28,29]. The product powder was then gradually annealed (10 K/min) to 870 K under high-vacuum conditions ($P < 10^{-5}$ mbar) and treated in vacuum for 2 h.

The resultant material was separated into two parts. The first part was oxidized with 3 Torr O_2 at 870 K to remove organic remnants from the precursor material. The second was oxidized with 3 Torr O_2 at 1070 K for the same reason and also to allow a crystal-phase transformation.

All supports were pretreated in a flow of 40 ml/min of pure O_2 for 5 h at 870 K before being impregnated with Pd salt. This was done mainly to remove some retained moisture from the supports, especially from the commercial support (P25). After this thermal treatment, the supports were impregnated with $Pd(NO_3)_2 \cdot 2H_2O$ (Merck) using the wet impregnation method. A ratio of 10 ml of water per gram of support was used, and the weight of the salt was calculated to obtain a final weight percentage of noble metal in the catalysts of 2. The resultant catalysts where then calcined at 770 K to remove nitrate and then gradually reduced (10 K/min) under a 50-ml/min flow of pure H_2 at different temperatures (298, 473, and 623 K) for 1 h.

Monometallic Pd/γ-Al_2O_3 and bimetallic Pd–Cu/γ-Al_2O_3 were synthesized using incipient wetness method, as described [18], using γ-Al_2O_3 (Sigma Aldrich) and the corresponding nitrate salts, $Pd(NO_3)_2 \cdot 2H_2O$ and $Cu(NO_3)_2 \cdot 3H_2O$ (Merck). The 5 wt% Pd catalyst was dried overnight at 373 K and calcined in air at 723 K. For the bimetallic catalyst, a subsequent impregnation was carried out with $Cu(NO_3)_2 \cdot 3H_2O$ using the same procedure; the resulting bimetallic catalyst was dried overnight at 373 K and calcined in air at 723 K. The catalyst was reduced for 1 h at 623 K in pure H_2. The final metal content of the catalysts was 5 wt% of Pd and 1.25 wt% of Cu. The bimetallic catalyst was synthesized for comparative purposes in kinetic measurements, because these catalysts are the most widely studied in the nitrate hydrogenation process. The metal content of the catalysts was evaluated by atomic absorbance spectroscopy (AAS) and found to be in agreement with the nominal values.

X-Ray diffraction (XRD) patterns were obtained using a Philips X'Pert PRO diffractometer (Bragg–Brentano θ/θ, geometry type). The Cu-K_α radiation source, a graphite (002) monochromator, provides continuous scans in the region $2\theta = 5$–$80°$, with a step size of 0.02° and a scan rate of 5 s/step.

The EPR sample cell, made of Suprasil quartz glass, was connected to an appropriate high-vacuum pumping system. It permitted thermal sample activation at $<10^{-5}$ mbar under dynamic vacuum conditions and reduction of the catalysts. The EPR spectra were recorded with a Bruker EMX 10/12-spectrometer system in the X-band mode. Measurements at 77 K were performed with an ER 4131 VT variable-temperature accessory. The presented spectra were obtained by accumulating 10–30 scans to obtain acceptable signal-to-noise ratios. The g values were determined on the basis of a DPPH standard. The electron center signal was measured at 77 K at a fixed-resonance magnetic field value for the respective EPR transitions.

Two sets of experiments were performed on the EPR. Each set consisted of a consecutive reduction of the calcined catalysts in 1 mbar of pure H_2. The temperatures used to perform the reductions were 298, 473, and 623 K. After reduction, one of the sets was allowed to cool in the presence of H_2 before the call was evacuated, whereas in the other procedure, the cell was evacuated at the temperature at which the reduction was carried out and cooled under dynamic vacuum. Cell evacuation took 10 min. O_2 (10 mbar) was dosed after each reduction step for both procedures to locate the particular species, because adsorbed oxygen strongly modifies the signals resulting from surface species [30].

Spin concentrations were estimated by numerical double integration of the first-derivative spectra and compared with a frozen Cu^{2+} aqueous solution, measured in an identical sample tube, as described elsewhere [31]. Thus a similar level of accuracy in the results is expected. Cu^{2+} provides a suitable comparison because it belongs to the same row as Ti and has the same number of unpaired electrons as Ti^{3+} (one unpaired electron); that is, both have $S = \frac{1}{2}$.

FTIR spectra were recorded on a Bruker IFS 28 with a resolution of 4 cm^{-1}. The spectrometer cell was connected to a vacuum system working in the 10^{-6} mbar range and to a heating system. The cell could be used for in situ pretreatment of samples, adsorption of gases, and measurements at low temperatures. The samples were pressed into self-supporting wafers, which were placed inside a ring furnace in the vacuum cell. CO adsorption measurements were carried out using 50 mbar of pure CO. The presented spectra were obtained at 100 K by accumulating 100 scans.

The catalysts were investigated after in situ consecutive reduction with 100 mbar of pure H_2 for 1 h, using the same temperatures of the EPR experiments, and cell evacuation for 30 min at the reduction temperature. Because the volume of the FTIR cell was greater than that of the EPR tube, the reductions were carried out with a higher hydrogen pressure for the latter, to normalize the number of moles of H_2 exposed to the catalyst for both experiments. The catalyst in calcined form was used as the starting material. Changes in the sample resulting from exposure to O_2 were also investigated. Catalysts were exposed to 10 mbar of pure O_2 at room temperature (290 ± 3 K) for 1 h. The cell was then evacuated for 15 min at same temperature before the samples were exposed to CO.

The activities and selectivities of the catalysts in the hydrogenation of nitrate ions were tested in a slurry thermostated batch reactor with a capacity of 1 l, equipped with a mechanical glass stirrer. In a typical run, 450 mg of the catalyst was charged into a reactor containing 0.75 l of distilled water. The content of the reactor was flushed first for 5 min with N_2 and then for 60 min with CO_2 and H_2. The reaction was started when a solution of nitrate salt was added to the vessel to achieve a concentration of 100 ppm of nitrates (KNO_3, Merck). A constant feed of CO_2 (100 ml/min) as a pH buffer and H_2 (90 ml/min) as a reducing agent were supplied using mass flow controllers. The reactions were carried out at atmospheric pressure, at 298 K, and using a stirring rate of 500 rpm. A typical kinetic run took 4 h.

The degradation of nitrates and the formation of nitrites and ammonia were measured at constant time intervals using high-performance liquid chromatography (HPLC) for $NO_3{}^-$ and $NO_2{}^-$ and a colorimetric test supplied by Merck for $NH_4{}^+$. The colorimetric tests were performed in a Shimadzu UV–vis spectrophotometer operating at $\lambda = 690$ nm, and the HPLC measurements were performed in a Spectra Physics device with an UV detector operating at $\lambda = 210$ nm. The column used was an IonoSphere 5A, and the mobile phase was a phosphate buffer with concentration of 0.02 mol and a pH of 5.3.

3. Results and discussion

3.1. XRD characterization

The percentages of each crystal phases present in each TiO_2 support investigated are summarized in Table 1. It can be seen that the anatase/rutile ratio for the sample P25 is almost 1, instead of the expected value of 3. This is because of the thermal treatment applied to the support before the impregnation with Pd. The temperature applied and the oxidizing characteristics of the treatment were sufficient to allow the phase transition of part of the anatase to rutile.

Table 1
Percentages of the crystal phases in the TiO_2

Catalyst	Reduction temperature (K)	Anatase (%)	Rutile (%)
Pd_P25 298	298	55	45
Pd_P25 473	473	55	45
Pd_P25 623	623	55	45
Pd_Ana 473	473	95	5
Pd_Ana 623	623	95	5
Pd_Rut 473	473	0	100
Pd_Rut 623	623	0	100

3.2. EPR characterization

EPR was performed to evaluate the formation of Ti^{3+} centers and their stability in the presence of O_2. Two sets of experiments were followed by EPR. In the first set, the catalysts were allowed to cool under an atmosphere of hydrogen after the in situ reduction. Fig. 1 shows the EPR spectra obtained for the catalysts Pd_P25. It should be emphasized that when the experiment was performed using Pd_Ana, similar results were observed (not shown). In contrast, no signals were observed with the pure supports in the absence of Pd. The spectra are very similar in term of both intensity and location of the signal for all reduction temperatures. The center of the main peak is located at $g = 1.995$ and is attributed to Ti^{3+} centers [30,32,33]. The g-tensor value was significantly higher than values normally reported for Ti^{3+} in solid TiO_2 ($g \approx 1.990$) [30,31], which would appear to be related to the presence of Pd. A similar effect on the g-tensor was observed by Huizinga et al. [34] for platinized TiO_2, where a value of 1.992 was measured and was attributed to Ti^{3+} formed in the vicinity of platinum clusters.

No perturbation in the intensity of the peaks was observed when 10 mbar of O_2 (not shown) was dosed. This insensitivity to oxygen, the narrow line width, and the high g-tensor value clearly indicate that the signal derives from bulk Ti^{3+} centers, that is, from trapped electrons in the support lattice. This implies a surface reoxidation as the Ti^{3+} centers generated are located at the surface. This process involves charge and/or mass transfer from the surface to the bulk. Because the transport of surface-reduced Ti cations to the bulk is largely unfavorable under the experimental conditions used [35], it is assumed that the process occurs through a charge transfer. Based on the present results, it is not possible to distinguish between interstitial and substitutional Ti^{3+}. Despite the extensive discussion of this issue, no agreement has yet been reached. Because this issue is be-

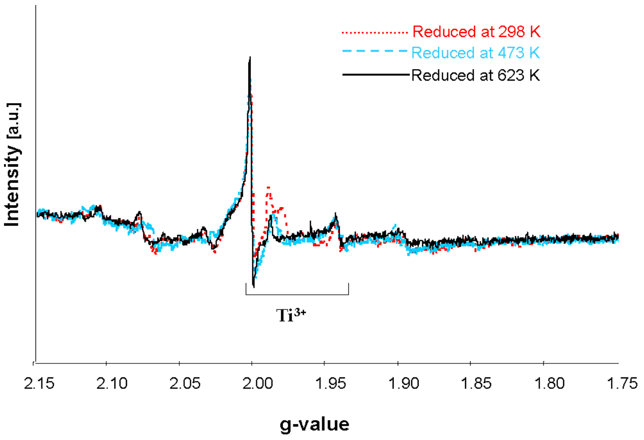

Fig. 1. EPR of Pd_P25 collected at 77 K, reduced at different temperature and cooled in 1 mbar of H_2.

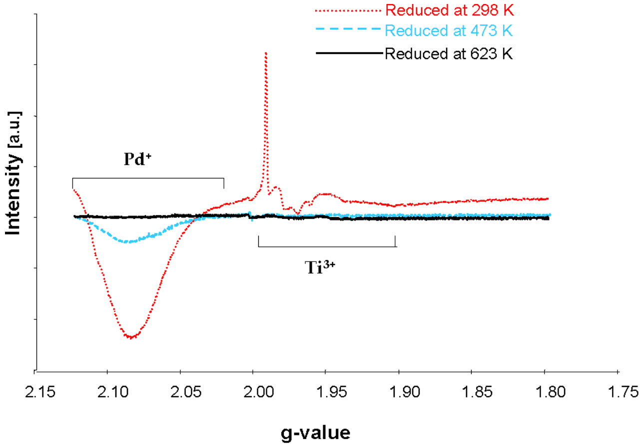

Fig. 2. EPR of Pd_Ana, collected at 77 K, reduced at different temperatures with 1 mbar of H_2 and evacuated before cooling.

yond the scope of the present work, we can conclude only that the Ti^{3+} centers have bulk characteristics and that they appear to be located in the vicinity of Pd.

In the second set of experiments, the cell was evacuated at the reduction temperature and the catalysts were cooled under dynamic vacuum. Fig. 2 shows the EPR spectra obtained for the catalysts Pd_Ana; the measurements made using Pd_P25 (not shown) gave similar results. The signal related to Ti^{3+} ($g = 1.991$) was measurable only when the catalysts had been reduced with 1 mbar of H_2 at 298 K and only when Pd was present. Another important observation was that the shape of the profiles remained the same after the catalysts were exposed to O_2 (not shown). The very narrow line width indicates that Ti^{3+} occupies a single type of site within the anatase. Following the foregoing reasoning, the Ti^{3+} centers are assumed to be present within the support lattice. In this set of experiments an additional signal was detected that was diminished in intensity with an increase in reduction temperature such that it remained undetected when the catalysts were reduced at 623 K. Because the g factor of the signal is significantly greater than 2, the signal must derive from another type of species, which in this case is assumed to be Pd, because no other chemical species are present in the catalysts. The signal is assigned to residual, incompletely reduced paramagnetic Pd^+ species. Furthermore, the catalyst color was visibly darker with an increase in the reduction temperature, indicating a reduction of Pd to its metallic state.

Any discussion of these results must begin by explaining why the support can be reduced at such low temperature. The explanation for this must be related to the presence of Pd in the catalysts. It is known that Pd promotes reduction of the support, allowing reduction to occur at a lower temperature [23]. This effect is due to the spillover of hydrogen and/or the presence of Pd β-hydride (absorbed hydrogen). Because these two mechanisms are possible, the question is which one is responsible for the formation of the Ti^{3+} centers measured?

Pd β-hydride is assumed to decompose at 343–363 K [21,36,37]. This implies that the presence of Pd β-hydride is possible only when the catalysts are cooled in an atmosphere of hydrogen (first set of experiments) and/or the catalysts are reduced and evacuated at 298 K (second set of experiments). These conditions are those under which Ti^{3+} center formation was observed. Therefore, it is proposed that Ti^{3+} center formation occurs mainly through hydride reduction rather then through hydrogen spillover. This does not invalidate the hypothesis of Ti^{4+} reduction by hydrogen spillover; however, under the conditions described here, its contribution was the less significant of the two processes.

During catalyst reduction, both adsorbed and absorbed hydrogen species are formed; both of these processes are reversible. Throughout the increase in temperature, the hydride (potentially the active species involved in the reduction of the support) dissolves [38,39], taking with it the electrons trapped at the Ti^{3+} centers. In the case that the catalysts are allowed to cool in hydrogen (first set of experiments), further formation of hydride is allowed, and the signal related to Ti^{3+} centers is observed. The insignificant increase in the signal with increased reduction temperature is an indication that the reduced support due to hydrogen spillover is not very pronounced. In the second series of experiments, hydride formation during cooling was prevented, and thus hydride decomposition occurred, leading to removal of the electrons trapped at Ti^{3+} centers, as confirmed by the disappearance of the signal related to Ti^{3+} centers when the catalysts were reduced and evacuated at higher temperatures.

For comparison, the spin concentrations resulting from the calculations using the frozen Cu^{2+} aqueous solution were 2.5×10^{19} spins/g catalyst for Pd_Ana and 3.1×10^{18} spins/g catalyst for Pd_P25. Using this rough estimation, it is possible to determine the percentage of support that was partially reduced under the experimental conditions applied. The values obtained were ∼0.4% for Pd_Ana and ∼0.1% for Pd_P25.

3.3. *Adsorption of CO on reduced Pd/TiO_2 catalysts*

FTIR measurements using CO as a probe molecule were performed to identify the species present on the surface of the catalysts, their oxidation states, and their susceptibility to the presence of oxygen in situ after reduction. Because of the weak nature of CO adsorption on exposed sites of the support, such as CO bonded to Ti^{3+} [40], experiments were conducted with the sample at 100 K. The results of the interactions of CO with the surface species of the catalysts supported on P25 and anatase after in situ reduction and evacuation are shown in Figs. 3a and b. The spectra in each figure were obtained for the same sample submitted consecutively to different reduction temperatures and CO adsorption. CO was previously evacuated at room temperature before subsequent reduction; thus it is assumed that the reduction procedures were identical for the FTIR and EPR experiments. Similar studies were also performed for

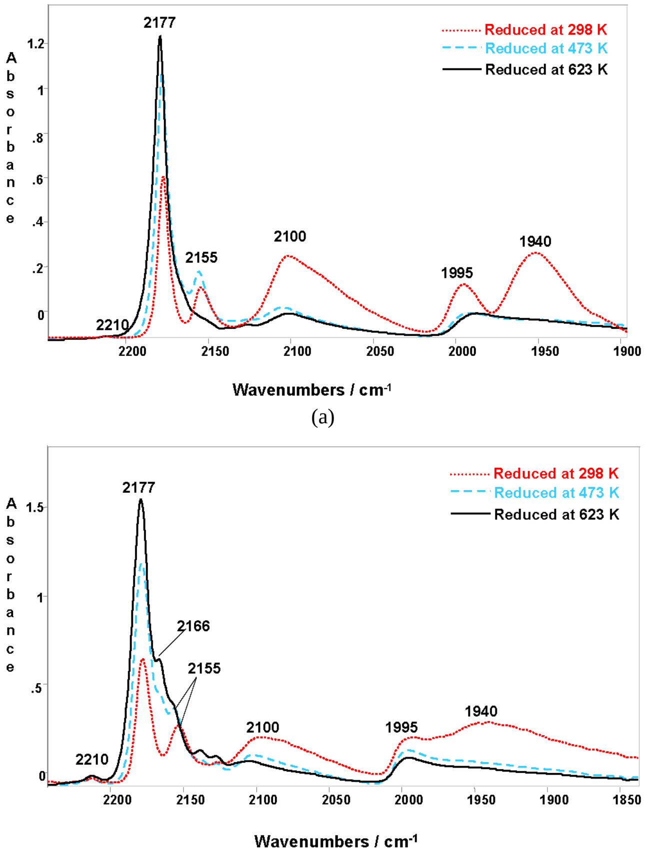

Fig. 3. FTIR spectra following exposure of samples (a) Pd_P25; and (b) Pd_Ana to 50 mbar of CO at 100 K, for samples reduced at different temperatures.

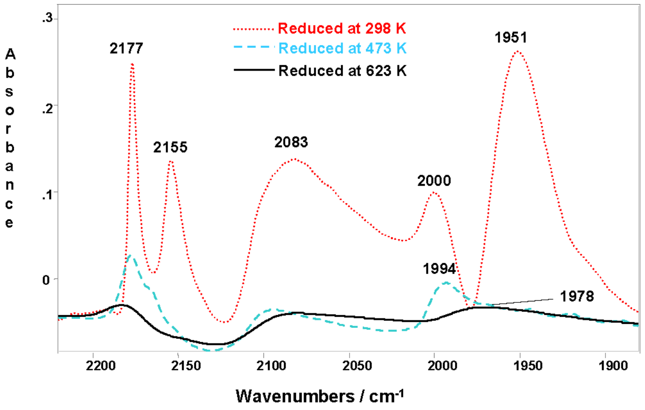

Fig. 4. Modifications to CO adsorption following exposure of the catalyst to 10 mbar of O_2. The spectra presented are the difference between the spectrum of CO adsorption before and after dosing of O_2. FTIR collected at 100 K and adsorption carried out with 50 mbar of CO on Pd_P25.

the supports in the absence of Pd (results not shown). Fig. 4 shows the perturbation in the intensity of bands due to adsorbed CO resulting from exposure to O_2.

Two features are evident in the spectra of the catalysts studied as a function of the increased reduction temperature: the increased intensity of the bands corresponding to adsorption on exposed Ti species (band centered at 2180 cm^{-1}) and the decreased intensity of bands related to adsorption of CO on exposed Pd sites (bands centered at 2100, 1995, and 1940 cm^{-1}). The band centered between 2176 and 2180 cm^{-1} is assigned to Ti^{4+}–CO β-acid sites [40–42], that is, five coordinated Ti ions. The shift of the band to high wave numbers with an increase in reduction temperature is related to dehydroxylation of the surface occurring during sample evacuation. It should be remembered that the catalysts were evacuated at the reduction temperature for 30 min to remove any water formed during the reduction process. The band was more pronounced in the presence of Pd. A slight decrease in band intensity was observed for samples containing Pd when the reduction was carried out at higher temperatures and exposed to oxygen. But in the case of the support alone, the intensity decreased strongly after the addition of oxygen. In the case of catalysts reduced at lower temperature (298 K), the band decreased by 30%. It is possible to conclude that the noble metal has two functions: promoting the formation of coordination vacancies and preventing their recombination with molecular oxygen.

A small band located at 2210 cm^{-1} was observed more clearly in spectra of the catalysts containing anatase as a support. This is attributed to another acidic cation, the α-Ti^{4+} acid sites [40,41], that is, four coordinated Ti ions or Ti with two coordination vacancies. Oxygen dosing had no effect on band intensity. Furthermore, this band was not observed for the support alone in the absence of the metal, which supports the argument that Pd promotes the development and stabilization of coordination vacancies. A consequence of the decreased coordination number of terminal Ti^{4+} is an increased surface positive charge of the catalysts. It should be mentioned that the interaction of CO with the α-Ti^{4+} is known to be much stronger and that its corresponding band intensity does not depend on the temperature at which the measurements were performed, whereas the intensity of the band representing the β sites has a temperature dependence (i.e., more intense when the measurements are performed at lower temperatures) [40].

The band between 2150 and 2158 cm^{-1} is assigned to CO adsorbed on Ti–OH [40]. The weak bands, which are visible in the spectra of the Pd/TiO_2 anatase catalyst at 2144 and 2138 cm^{-1}, can be related to the same sites but with slightly different environments. They are apparent with greater intensity then normally expected, because the measurements were performed at low temperature. These features decreased with increasing reduction temperature due to the dehydroxylation process. The final band, which can be attributed to adsorption at exposed Ti cations, is located at 2166 cm^{-1} and is assigned to Ti^4–$(CO)_2$ species [40]. This band was observed only in the sample containing anatase as a support.

For spectra of catalysts containing Pd, three different types of adsorbed species due to the interaction of CO with different Pd sites can be identified. The highest-frequency band at 2100 cm^{-1} is attributed to CO linearly bonded to Pd [24,40,43]. Bands at 1995 and 1940 cm^{-1} are assigned to compressed and isolated bridge carbonyls, respectively [24, 40,43,44]. All bands decreased in intensity with increasing reduction temperature. The decreased number of exposed Pd sites available for CO adsorption could be a consequence of the onset of strong metal support interaction (SMSI) and/or a sintering process.

The term SMSI was first proposed by Tauster et al. [45,46] to indicate the modification of the adsorption ability of metals from groups 8, 9, and 10 when supported on partially reducible oxides such as TiO_2 and reduced at elevated temperatures (generally 773 K). The standard criterion for SMSI is a significant reduction in H_2 or CO adsorption capacity with elevated reduction temperature without an accompanying increase in crystallite size [23,45,46].

The SMSI phenomenon can be explained either by the decoration of the metal surface with partially reduced oxides [47–53] or by an electron transfer process between the support and the dispersed metal [47,54,55]. Both of these situations lead to decreased chemisorbtion of CO on the metal. In the first situation this is due to the decrease in the surface metal atoms, whereas in the second it is due to electronic modification, which leads to a weakened adsorbate–adsorbent bond.

In the present study, FTIR measurements of chemisorbed CO were carried out at 100 K, which facilitates CO adsorption and maximizes coverage, as confirmed by the appearance of bands due to CO bonded to some Ti species, which are otherwise highly unstable at room temperature [40]. Under these experimental conditions, diminished intensity of bands due to adsorbed CO is thus not expected should SMSI manifest itself in terms of an electron transfer process leading to weakened adsorption. It is more likely that the diminished CO uptake, as indicated by the reduced intensity of CO absorption bands with increasing reduction temperatures, is a consequence of the SMSI state, which in this case results from decoration of Pd particles by partially reduced TiO_2.

Sintering is expected to play at most a minor role in reduced CO uptake; this is based on the assumption that the catalysts were previously calcined at a temperature above the palladium Tammann temperature ($T = 593$ K, $T \sim 0.5T_{\mathrm{mpt}}$) [56,57], which would be expected to lead to a greater degree of sintering than occurs during the reduction procedure. An acceptable criterion for the occurrence of sintering is that the treatment temperature is above the Tammann temperature. In only one case was the reduction temperature sufficiently high for sintering to occur on the basis of this criterion. Furthermore, there was no increase in the ratio between bridge CO and linear CO carbonyls on Pd, which could also be interpreted in terms of morphological changes that generally accompany any particle growth process [24].

Establishment of the catalyst system in an SMSI state allows stabilization of the generated coordination vacancies or acidic sites of Ti, which is not expected in the absence of strong interactions between metal and support. This is illustrated in Fig. 5, where the dosing of oxygen leads to only minor decreases in the bands due to the interaction of CO with exposed Ti species when the samples are considered in the SMSI state (473 and 623 K), whereas for the support in the absence of metal, band intensity decreased by around 30%.

Before concluding the characterization section, we note that FTIR measurements were not possible for the rutile supported catalysts using the methodology applied for the other two types of catalyst. This failure was related to the difficulty in obtaining adequate IR transmission through the sample after the reduction pretreatments. Therefore, we present no characterization for this type of catalyst. However, for the sake of providing a useful comparison in terms of the role of the support, we conducted activity measurements using these samples.

3.4. Catalytic performance

The results of activity measurements, maximum nitrite concentration, and selectivity of the catalysts to nitrogen are plotted in Figs. 5a–c, with values summarized in Table 2. The overall degradation profiles of nitrate via nitrite to nitrogen and ammonium over all catalysts are compared in Fig. 6. The activities were calculated from the slope of the initial linear section of the conversion curve (up to 20 min reaction time); the selectivities were calculated using the ammonium concentration remaining at the end of the catalytic test (4 h).

The TiO_2-supported catalysts displayed a relatively high activity for the removal of nitrates. In some cases, higher values than those of the reference PdCu bimetallic catalyst were obtained. These results are surprising given literature reports that TiO_2 might be less promising as a support [6]. Another important observation is that the nitrite concentration was very low or reached undetectable levels for the monometallic catalysts. The final concentration of $NO_2{}^-$ was 0 for all catalysts except Pd_Ana623 (Table 2), for which a level of 0.3 ppm was recorded. According to the reaction mechanism proposed by Wärnă et al. [13], nitrates are reduced in a stepwise fashion, initially to nitrites over bimetallic sites, before migrating to monometallic sites where subsequent nitrite reduction takes place. Generally, this two-step process leads to a release of $NO_2{}^-$ into the solution, which may be further reduced at a later stage. In this way a potentially relatively high concentration of nitrites in solution during reaction might exist for the bimetallic catalysts, consistent with data given here for the PdCu sample (Fig. 5b). Because the final nitrite concentration was either very low or mostly undetectable for the monometallic catalysts (Table 2), and the maximum obtained (Fig. 5b) were also very low for these samples, we assume that the active sites for the reduction of nitrates to nitrites are the same as for subsequent steps (nitrites toward nitrogen or ammonium) and that in general, the release of nitrites into solution followed by subsequent reduction is not the predominant pathway.

As mentioned earlier, the accepted mechanism for the reduction of nitrates to nitrites requires promotion of the noble metal by addition of a second metal, that is, a bimetallic site,

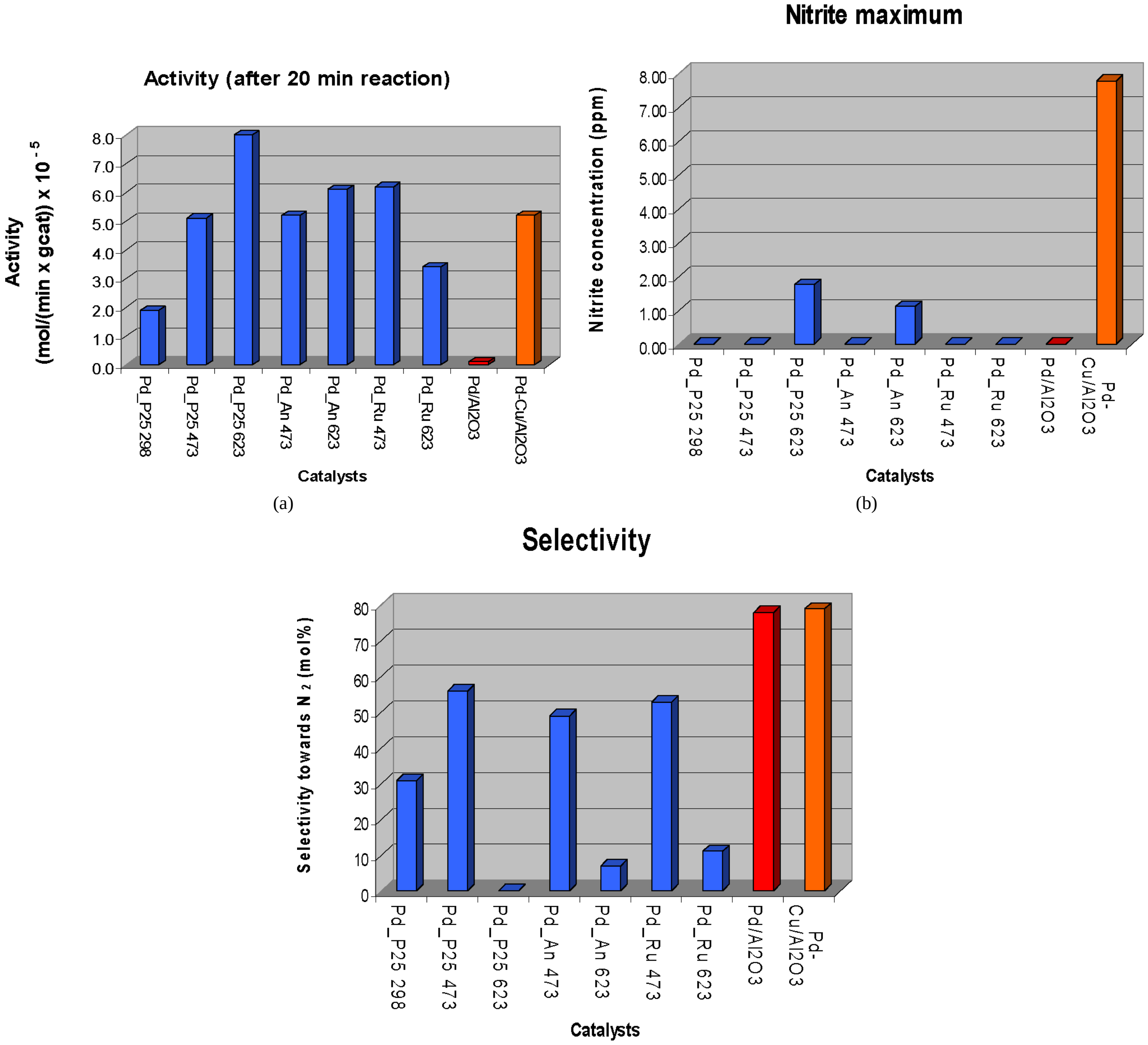

(a) (b)

(c)

Fig. 5. Catalytic performances of the catalysts: (a) activity (after 20 min reaction); (b) maximum concentration of NO_2^-; (c) selectivity to N_2.

Table 2
Activity and selectivity of the different catalysts in the hydrogenation of 100 ppm nitrates

Catalyst	Activity (mol/(min g_{cat})) × 10^{-5}	$[NO_2^-]_{max}$ (ppm)	$[NO_2^-]_f$ (ppm)	Selectivity towards N_2 (mol%)
Pd_P25 298	1.9	0.0	0.0	31
Pd_P25 473	5.1	0.0	0.0	56
Pd_P25 623	8.0	1.76	0.0	0
Pd_Ana 473	5.2	0.0	0.0	49
Pd_Ana 623	6.1	1.1	0.3	7
Pd_Rut 473	6.2	0.0	0.0	53
Pd_Rut 623	3.4	0.0	0.0	11
Pd/γ-Al_2O_3	0.1	0.0	0.0	78
Pd-Cu/γ-Al_2O_3	5.2	7.8	0.0	77

$[NO_2^-]_{max}$, maximum nitrite concentration observed during the run; $[NO_2^-]_f$, final nitrite concentration.

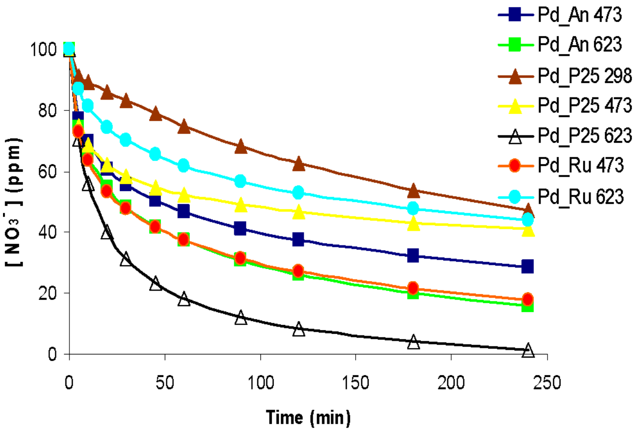

Fig. 6. Nitrates conversion profiles as a function of time for all catalysts.

because monometallic catalysts supported on Al_2O_3 show poor activity [18] (Table 2). Previous studies [18,58] have demonstrated that nitrates might be reduced to nitrites on metallic copper according to a redox reaction, leading to the oxidation of copper species. Subsequently, the role of the noble metal is to activate hydrogen and enable copper reduction. A similar type of mechanism could well be envisaged here; however, in this case the promoting role of the noble metal involves generation/stabilization of reduced species of the titanium support.

After nitrates are introduced to a solution, they are adsorbed at exposed acid sites (oxygen vacancies) of the support through electrostatic interactions. These sites are expected to be located in the vicinity of the Pd particles, because otherwise it is difficult to envisage a scenario in which they would have the required stability. A similar type of adsorption site has been postulated by Epron et al. [22].

Because nitrate degradation is a reduction process, the transfer of electrons is an integral part of the reaction scheme. These electrons are envisaged as being located at the Ti^{3+} centers, generated by the catalyst from the Pd β-hydride during the flushing of the reaction mixture with hydrogen before the introduction of nitrates. These centers are extremely reactive; however, EPR evidence suggests that they are located within the lattice of the support, which would make them inaccessible for the reaction unless they were conducted to the surface, where reaction could take place. Whether electrons are transferred from the support directly to the NO_3^- or primarily to the metal and from this to the anion is an open question. The charge transfer from the support to the metal has been the subject of discussion, with the suggestion that the electronic interactions present in a SMSI state could result in a charge transfer from the support to the metallic particles [47]. Kim et al. [59] observed a shift in the Pd XRD peak for Pd/TiO_2 reduced at 773 K, which they attributed to negative charge transfer from Ti^{3+} to the Pd particles.

It seems plausible that the charge transfer is occurring during the reaction; however, the catalytic results cannot be fully accounted for if this is the only pathway considered. The activity is increased with increasing temperature at which the catalysts were reduced (except where rutile was used as the support); however, the EPR results show only a minor increase in the Ti^{3+} signal when the reduction temperature was increased. Therefore, it is assumed that another parallel process is occurring.

FTIR experiments confirm the presence of the SMSI condition and also suggest that it is related to a decoration of Pd particles by partially reduced TiO_2 suboxide species. The chemical structure of the partially reduced TiO_2 is believed to be Ti_4O_7 [39] from studies using electron diffraction and lattice spacing measurements. This Ti_4O_7 phase was detected during reduction of the TiO_2 support, which was not observed in the absence of Pt. This electronically enriched local structure contains potential active sites for nitrate reduction. In fact, the development of an SMSI state, apart from the enhanced support Lewis acid site density, was the only significant change observed with an increase in reduction temperature. It can be assumed that the development of the SMSI state was directly related to the increased activity, despite a reduction in the total number of exposed metal surface sites. This apparent paradox regarding activity enhancement due to formation of an SMSI state but a reduction in the total number of sites is not without precedent [26,60].

Tacke and Vorlop [7] found the reaction order to be 0.7 with respect to nitrate and independent of hydrogen partial pressure, provided that the latter pressure was >1.0 bar. Pintar et al. [9] suggested that the reaction was first order at lower nitrate concentrations and zero order at higher concentrations, which is an indication that nitrate adsorption follows a Langmuir-type process at the respective active centers on the catalyst surface. Therefore, a great excess of metal sites would be expected for the reduction of nitrates. SMSI is expected to lead to only a decreasing number of potential active sites, not to poisoning of the catalyst. The possibility that the remaining sites were much more active and/or that new, active sites (e.g., at the Pd–support interface) were created should not be discounted [25].

The rate-determining step in the nitrate conversion process is the reduction of nitrates to nitrite. In this case this step is controlled by generation of the Ti^{3+} centers, because in the nitrate reduction profiles for these catalysts, a steep decrease in concentration is observed during the initial stages of the reaction. This decrease appears to be related to the rapid consumption of previously stabilized electrons, followed by hydroxylation of the acid sites, and a significant decrease in the activity beyond that expected for a first-order consumption of nitrate from the reaction media.

In terms of catalyst selectivity, the catalysts supported on TiO_2 exhibit relatively poor selectivity, which can be justified by the known strong hydrogenation character of this type of catalyst as well as the fact that high activity is often compensated by poorer catalyst selectivity, due in this case to overreduction. Furthermore, the results indicate that the overall reaction is not strongly dependent on the amount of nitrite accumulated in the liquid phase, as has been suggested for the bimetallic catalysts [61]. The poisoning resulting from using a solution buffer (CO_2) is not as relevant as in the case reported for Pd/CeO_2 [22]. This finding is significant, because it offers opportunities for the design of further catalyst development based on titanium with the objective of improving the nitrogen selectivity of these catalysts.

The other important topic relevant to the present discussion is the structure dependence of the activity. We observe that all catalysts are active, although not to the same extent. In the case of the anatase and P25 (mixed-phase) structures, increased activity with increasing reduction temperature was observed. This is assigned to increased Lewis acidity of the support, which enhances the initial adsorption of the nitrate ions. For rutile, different behavior was observed that may be related to the reduction temperature, although further speculation is not desirable at this stage, because performing the IR measurements for these samples was not possible. Somewhat surprising was the finding that the highest values for activity were obtained for the catalysts supported on P25, not those supported on the pure anatase, which would suggest further degrees of complexity in terms of the optimum support structure/exposed crystal planes. This is an extremely complex topic of discussion and beyond the scope of the present work; however, we believe that the boundaries between the crystal structures may act as electron-trapping sites involved in the reduction process.

4. Conclusion

In answer to the question raised in this paper's title, TiO_2 would appear to promote the reaction leading to removal of nitrates from aqueous sources. The reaction mechanism consists of two parallel processes catalyzed by an excess of electrons trapped by the support, in the form of either Ti^{3+} centers or partially reduced support in intimate contact with Pd crystallites (SMSI). Decreased amounts of adsorbed CO were measured when the reduction temperature was increased as a consequence of the SMSI state, whereas EPR measurements confirmed the presence of Ti^{3+} centers at 298 K (reaction temperature), possibly resulting from the generation of Pd β-hydride species. The SMSI state allowed a stabilization of the Lewis acidic cus species. Monometallic catalysts showed a low selectivity to undesired nitrites throughout the reaction, indicating that these intermediates are rapidly reduced, possibly in a single site mechanism, unlike the bimetallic PdCu samples, in which nitrite ions are initially released into solution before being reduced in a second step. Overreduction to ammonia resulted in a poorer selectivity to nitrogen for the titanium-based Pd monometallic samples than for the bimetallic analogues. However, the high activity exhibited by Pd/TiO_2 opens up new opportunities in the design of catalysts for the denitration process.

Acknowledgments

The work was partially supported by the Fonds zur Förderung der Wissenschaftlichen Forschung under Project FWF P13521. The authors thank Dr. Erich Halwax of the Institut für Chemische Technologien und Analytik of Vienna University of Technology for performing the XRD measurements and the College of Physical Sciences, University of Aberdeen for providing a postgraduate research studentship (to J.S.).

References

[1] L.W. Canter, Nitrate in Groundwater, CRC Press, Boca Raton, FL, 1997.
[2] K.-D. Vorlop, T. Tacke, M. Sell, G. Strauss, European Patent DE 3830850 A1 (10 September, 1988).
[3] T. Tacke, K.-D. Vorlop, Dechema Biotechnology Conferences, vol. 3, VCH, Weinheim, 200X.
[4] K.-D. Vorlop, T. Tacke, Chem. Ing. Technol. 61 (1989) 836, (1989) 1007.
[5] K.-D. Vorlop, S. Hörold, K. Pohlandt, Chem. Ing. Technol. 64 (1992) 82.
[6] S. Hörold, K.-D. Vorlop, T. Tacke, M. Sell, Catal. Today 17 (1993) 21.
[7] T. Tacke, K.-D. Vorlop, Chem. Ing. Technol. 65 (1993) 1500.
[8] G. Strukul, R. Gavagnin, F. Pinna, E. Modaferri, S. Perathoner, G. Centi, M. Marella, M. Tomaseli, Catal. Today 55 (2000) 139.
[9] A. Pintar, J. Batista, J. Levec, T. Kajiuchi, Appl. Catal. B 11 (1996) 81.
[10] A.J. Lecloux, Catal. Today 53 (199) 23.
[11] U. Prüsse, K.-D. Vorlop, Catal. Today 55 (2000) 79.
[12] F. Deganello, L.F. Liotta, A. Macaluso, A.M. Venezia, G. Deganello, Appl. Catal. B 24 (2000) 265.
[13] J. Wärnă, I. Turunen, T. Salmi, T. Maunula, Chem. Eng. Sci. 49 (1994) 5763.
[14] S. Naïto, M. Tanimoto, J. Catal. 119 (1989) 224.
[15] F. Epron, F. Gauthard, C. Pinéda, J. Barbier, J. Catal. 198 (2001) 309.
[16] S. Kerkeni, E. Lamy-Pitara, J. Barbier, Catal. Today 75 (2002) 35.
[17] A. Pintar, Catal. Today 77 (2003) 451.
[18] J. Sá, H. Vinek, Appl. Catal. B 57 (2004) 247.
[19] J. Sá, S. Gross, H. Vinek, Appl. Catal. A, submitted for publication.
[20] J. Sá, D. Gasparovicova, K. Hayek, E. Halwax, J.A. Anderson, H. Vinek, Catal. Lett., submitted for publication.
[21] R. Gavagnin, L. Biasetto, F. Pinna, G. Strukul, Appl. Catal. B 38 (2002) 91.
[22] F. Epron, F. Gauthard, J. Barbier, J. Catal. 206 (2002) 363.
[23] Y. Li, B. Xu, Y. Fan, N. Feng, A. Qui, J.M.J. He, H. Yang, Y. Chen, J. Mol. Catal. A 216 (2004) 107.
[24] J.H. Kang, E.W. Shin, W.J. Kim, J.D. Park, S.H. Moon, J. Catal. 208 (2002) 31.
[25] J. Silvestre-Albero, A. Sepúlveda-Escribano, F. Rodrígues-Reinoso, J.A. Anderson, J. Catal. 223 (2004) 179.
[26] J.D. Bracey, R. Burch, J. Catal. 86 (1984) 384.
[27] S. Brunauer, P.H. Emmet, E. Teller, J. Am. Chem. Soc. 60 (1938) 309.
[28] S. Benfer, E. Knozinger, J. Mater. Chem. 9 (1999) 1203.
[29] D.M. Schleich, B. Walter, Nanostruct. Mater. 8 (1997) 579.
[30] R.F. Howe, M. Grätzel, J. Phys. Chem. 91 (1987) 3906.
[31] R.F. Howe, M. Grätzel, J. Phys. Chem. 89 (1985) 4495.
[32] D.C. Hurum, A.G. Agrios, K.A. Gray, T. Rajh, M.C. Thurnauer, J. Phys. Chem. B. 107 (2003) 4545.
[33] P. Meriaudeau, M. Che, P.C. Gravelle, S. Teichner, Bull. Soc. Chim. France 1 (1971) 13.
[34] T. Huizinga, R. Prins, J. Phys. Chem. 85 (1981) 2156.

[35] M.A. Henderson, Surf. Sci. 343 (1995) L1156.
[36] J. Batista, A. Pintar, D. Mandrino, M. Jenko, V. Martin, Appl. Catal. A 206 (2001) 113.
[37] T.-C. Chang, J.-J. Chen, C.-T. Yeh, J. Catal. 96 (1985) 51.
[38] M. Boudart, H.S. Hwang, J. Catal. 39 (1975) 44.
[39] R.T.K. Baker, E.B. Prestridge, G.B. McVicker, J. Catal. 89 (1984) 422.
[40] K.I. Hadjivanov, G.N. Vayssilov, Adv. Catal. 47 (2002) 307.
[41] C. Morterra, J. Chem. Soc., Faraday Trans. 1 84 (1988) 1617.
[42] V. Bolis, B. Fubini, E. Garrone, C. Morterra, J. Chem. Soc., Faraday Trans. 1 85 (1989) 1383.
[43] D. Tessier, A. Rakai, F. Bozon-Verduraz, J. Chem. Soc., Faraday Trans. 88 (1992) 741.
[44] K. Choi, M.A. Vanice, J. Catal. 127 (1991) 465.
[45] S.J. Tauster, S.C. Fung, R.L. Garten, J. Am. Chem. Soc. 100 (1978) 170.
[46] S.J. Tauster, S.C. Fung, J. Catal. 53 (1978) 29.
[47] R. Green, P. Morrall, M. Bowker, Catal. Lett. 98 (2004) 129.
[48] J. Santos, J. Phillips, J.A. Dumesic, J. Catal. 81 (1983) 147.
[49] H.R. Sadeghi, V.E. Henrich, J. Catal. 87 (1984) 279.
[50] A.J. Simoens, R.T.K. Baker, D.J. Dwyer, C.R.F. Lund, R.J. Madon, J. Catal. 86 (1984) 359.
[51] Y.-W. Chung, G. Xiong, C.C. Kao, J. Catal. 85 (1984) 237.
[52] C.S. Ko, R.J. Gorte, J. Catal. 90 (1984) 59.
[53] G.B. Raupp, J.A. Dumesic, J. Catal. 95 (1987) 587.
[54] J.M. Herrmann, M. Gravelle-Rumeau-Maillot, P.C. Gravelle, J. Catal. 104 (1987) 136.
[55] P. Chou, M.A. Vannice, J. Catal. 104 (1987) 1.
[56] N.M. Rodriguez, S.G. Oh, R.A. Dalla-Betta, R.T.K. Baker, J. Catal. 157 (1995) 676.
[57] P.O. Thevenin, E. Pocoroba, L.J. Petterson, H. Karhu, I.J. Väyrynen, S.G. Järas, J. Catal. 207 (2002) 139.
[58] A. Edelmann, W. Schießer, H. Vinek, A. Jentys, Catal. Lett. 69 (2000) 11.
[59] W.J. Kim, J.H. Kang, I.Y. Ahn, S.H. Moon, Appl. Catal. A 268 (2004) 77.
[60] S.Y. Wang, S.H. Moon, M.A. Vannice, J. Catal. 71 (1981) 167.
[61] A. Pintar, T. Kajiuchi, Acta Chim. Slovenica 42 (1995) 431.